



## Performance of METRIC in estimating hourly and daily evapotranspiration fluxes over an irrigated field in Saudi Arabia

Rangaswamy Madugundu<sup>1</sup>, Khalid A. Al-Gaadi<sup>1,2</sup>, ElKamil Tola<sup>1</sup>, Abdalhaleem A. Hassaballa<sup>1</sup>, Virupakshagouda C. Patil<sup>1</sup>

5 <sup>1</sup>Precision Agriculture Research Chait, King Saud University, Riyadh, 11451, Saudi Arabia

<sup>2</sup>Department of Agricultural Engineering, College of Food and Agriculture Sciences, King Saud University, Riyadh, 11451, Saudi Arabia

*Correspondence to:* Rangaswamy Madugundu (rmadugundu@ksu.edu.sa)

**Abstract.** Accurate estimation of evapotranspiration (ET) is essential for hydrological modelling and efficient crop water management in hyper-arid climates, like the one in the Eastern Region of Saudi Arabia. Therefore, a study was designed to apply the METRIC algorithm on Landsat-8 images, acquired from June to October 2013, for the development of ET maps for a 50-ha center pivot irrigated alfalfa field. The METRIC estimated energy balance components and ET were evaluated against the data provided by an Eddy Covariance (EC) flux tower installed in the field. Results indicated that the METRIC algorithm provided accurate ET estimates over the study area, with RMSE values of 0.09 mm h<sup>-1</sup> and 0.38 mm d<sup>-1</sup>. The METRIC algorithm was observed to perform a relatively better in full canopy conditions compared to that in partial canopy conditions. On the average, the METRIC algorithm overestimated the hourly ET by 6.6% in comparison to the EC measurements; however, the daily ET was underestimated by 4.2%.

**Keywords.** Arid region, energy balance, eddy covariance, landsat-8

### 1 Introduction

20 In the Kingdom of Saudi Arabia (KSA), which suffers from severe water shortage problems, the agricultural sector was estimated to consume about 85% of the total freshwater used in 2008 (Al-Kahtani and Ismaiel, 2010), which increased to 90% by 2012 (Elnesr and Alazba, 2013). With the limited water resources and to fulfill the needs of the increasing population in the KSA, efficient use of water for crop production is essential (Hussain et al., 2010; Praveen et al., 2012). Various studies (Kassem and Al-Moshileh, 2008; Atta et al., 2011; Al-Ghobari et al., 2013; Mohammad et al., 2013) recommended advanced irrigation systems for improving agricultural water use efficiency in the Kingdom. As an example, a reduction in the irrigation water of 30–40% was attained through sprinkler irrigation compared to traditional methods, and an additional saving of 10–25% can be reached with drip irrigation systems (Rizaiza and Al-Osaimy, 1996). Furthermore, implementation of recent innovative precision irrigation technologies, in conjunction with the accurate estimation of crop water requirements through remotely sensed data, can significantly enhance the efficient use of irrigation water in the agricultural sector.



Evapotranspiration (ET) measurements are recognized as an essential prerequisite for various water management applications such as irrigation scheduling, hydrologic modelling, nutrient cycles and drought monitoring (Bastiaanssen et al., 2000; Allen et al., 2005; Chavez et al., 2005; Senay et al., 2008; Santos et al., 2010; Anderson et al., 2012; Mkhwanazi and Chavez, 2012; Gowda et al., 2013; Lagos et al., 2013; Moorhead et al., 2013; Yee et al., 2014). In semiarid climates, ET can significantly influence the hydrologic cycle through the crop water use. Therefore, an accurate determination of ET is considered as one of the crucial and essential factors influencing the optimal management of crop water use through different irrigation systems (Hoedjes et al., 2008). On the other hand, the accurate determination of energy balance elements such as sensible heat (H), soil heat (G) and latent heat (LE) fluxes is of great importance for water management practices, especially in arid and semi-arid regions (Zeweldi et al., 2010). Estimation of ET has been performed through different direct/indirect methods including the lysimeter, water balance, Bowen Ratio (BR), Eddy Covariance (EC), scintillometer and Remote Sensing (RS) techniques (Allen et al., 2011a; Rana and Katerji, 2000). Among all the methods used for the estimation/measurement of ET, only lysimeter and EC methods can provide direct measurements of LE or ET; while, other methods use certain equations and assumptions to estimate heat fluxes using measurable parameters (FAO, 1977; Drexler et al., 2004; Chavez et al., 2009a).

Recently, EC systems have gained a lot of popularity in the determination of ET. Several studies have been conducted to investigate the effectiveness of the EC systems in estimating accurate values of H, LE and ET. As an example, Chavez et al. (2009b) conducted a study to investigate the accuracy of the EC measured energy balance components (H and LE) compared to those measured by the large weighing lysimeter on an irrigated cotton field in the USA. Their results showed that the mean values of the EC-measured H and LE were underestimated by about 30% compared to those measured by the lysimeter method. However, adjusting the EC data, through the techniques of energy closure and BR, contributed significantly to improving the accuracy of the ET values measured by the EC system. Ding et al. (2010) compared the EC measured ET ( $ET_{EC}$ ) with the lysimetric data ( $ET_L$ ) for maize in 2009. Their results showed a non-closure ratio of 0.84 of the energy balance for the daytime fluxes. However, the forced energy balance closure with BR data improved the accuracy from 79.2% to 95.2%. Therefore, the ET values measured by the EC system need to be adjusted, through an appropriate method, to improve their accuracy.

In-situ point measurements provide accurate ET values; however, these methods are limited to small areas only. An alternative method is to use numerical models, which are successfully used in assessing the spatial distribution of ET on larger scales. However, the process of obtaining accurate estimates of ET, using these computational models, requires the access to high-quality meteorological data. Based on the fact that most of the methods employed to accurately estimate ET provide only point measurements, and therefore, not suitable for applications in large areas, the development of new techniques for continuous determination of ET over large agricultural areas are of great importance. RS systems can provide a sound basis for the development of such technologies (Bala et al., 2013). RS techniques have significantly contributed to the provision of different methods used for the estimation of the spatial ET over large areas, which is hard to achieve by conventional methods (Farah et al., 2004; Colaizzi et al., 2006).



Different methods of RS systems have been successfully implemented to estimate the spatially distributed ET values over agricultural fields (Kalma et al., 2008; Gowda et al., 2008). One of the RS models, most commonly used for the determination of ET values, is the Surface Energy Balance Algorithm for Land (SEBAL) with an estimation accuracy ranging from 67% to 97%. Recently, several SEBAL based models have been developed and successfully implemented in  
5 different water management practices (Paul et al., 2013). Examples of such models include the Mapping Evapotranspiration at high Resolution and with Internalized Calibration (METRIC), Modified SEBAL (M-SEBAL), Simplified Surface Energy Balance (SSEB), Remote Sensing of Evapotranspiration (ReSET), Surface Energy Balance System (SEBS) and Surface Energy Balance with Topography Algorithm (SEBTA). The METRIC model, which was developed to determine the quantity and spatial distribution of ET over large areas, is considered as one of the most appropriate models for the  
10 continuous estimation of ET over crops during the growing season (Allen et al., 2007; Patil et al., 2015).

Accurate estimation of ET is critical for crop water management, especially under hyper-arid climates with scarce freshwater resources, as in the KSA. Long-term spatial and temporal ET measurements are not yet available in the Kingdom. Therefore, the main goal of this study was to employ the Eddy Covariance (EC) system for the assessment of the performance of the METRIC model, which is based on satellite data, in estimating the hourly- and daily-based ET over a  
15 center pivot irrigated alfalfa field.

## 2 Materials and Methods

### 2.1 Study area

The study was carried out on a 50-ha alfalfa field, which was one of the 48 agricultural fields of Todhia Arable Farm (TAF) located about 250 km Southeast of Riyadh, the capital city of Saudi Arabia, at coordinates of 24° 11' 00" E and 48° 56' 14.6"  
20 N (**Figure 1**). The farm was under an arid climate with hot summers ( $40 \pm 2$  °C) and cold to moderate winters ( $15 \pm 3$  °C) and a mean air temperature of 35°C. The annual rainfall was about 90 mm, most of which occurred in the period from November to February. Due to the high crop water demand combined with the highly erratic rainfall, irrigation is entirely provided using underground water delivered by center pivot irrigation systems. The major crops cultivated in the study area were alfalfa, Rhodes grass and corn.

### 25 2.2 Eddy Covariance (EC) system

Eddy Covariance system (LI-COR, Lincoln, NE, USA) was installed, on May 27th, 2013, over the selected alfalfa field. The EC flux tower was equipped with response sensors, including an open-path gas analyzer (Licor, LI-7500), a 3-axis ultrasonic anemometer (GILL), a net radiometer (CNR-4), soil heat flux plates, pyranometer and a quantum sensor. The EC measurements were recorded at the height of 3.67 m above the soil surface.

30 The recorded EC data, for the period from June to October 2013, was used for this study. Flux computations were performed using Eddypro software program (ver. 5.0). During the process, the collected 30-minute data sets were subjected



to raw data processing, such as wind speed measurement offsets, axis rotation for tilt correction, de-trending turbulent fluctuations, time lag optimization settings, spectral corrections and footprint estimation following the procedures described in the Eddypro software instruction manual (LI-COR). As the sonic anemometer was tilted 243° towards the North, an angle-of-attack correction for wind components was also performed. During the filtering process, EC data was excluded whenever there was a condensation, a covariance with missing values (-9999) or periods with incorrect sonic temperatures (i.e. >50 °C). The missed data was filled with the standard methods as described in the manual (LI-COR). Subsequently, the processed EC data was used in the computation of the ET (i.e.  $ET_{EC}$ ).

### 2.3 Satellite images

Eight cloud free Landsat-8 (OLI/TIRS) satellite images (Path 165, Row 43) were downloaded for the study period (June to October 2013) from the United States Geological Survey (USGS) Earth Explorer site (<http://earthexplorer.usgs.gov>), **Table 1**. The downloaded data was georeferenced to the Universal Transverse Mercator (UTM) Map projection using the World Geodetic System 84 (WGS84) datum. Subsequently, Fast Line-of-sight Atmospheric Analysis of Hypercubes (FLAASH) algorithm in ENVI software was used to convert Landsat-8 digital numbers to Top-Of-Atmosphere (TOA) spectral reflectance. Also, land surface temperature (LST) layers were generated using split window algorithm (USGS). The obtained spectral reflectance and the land surface temperature values were utilized as inputs for the ET estimation employing the METRIC algorithm. Image analysis and the execution of the METRIC algorithm were performed using ENVI software program (ver. 5.1).

### 2.4 METRIC algorithm and ET estimation

The METRIC algorithm has been developed exclusively for the estimation of ET from Landsat data (Allen et al., 2005). A total of eight Landsat-8 images were processed and used for the estimation of ET ( $ET_{METRIC}$ ) over the experimental alfalfa field. During the  $ET_{METRIC}$  computation, surface characteristics such as surface albedo, vegetation indices, surface emissivity and surface temperature were estimated as intermediate products. Anchor pixels (hot and cold) were selected, and the energy components such as the net radiation ( $R_n$ ), the soil heat flux ( $G$ ) and the sensible heat flux ( $H$ ) were estimated as well. Finally, the latent heat flux (LE) was predicted as a residual of the land surface balance (Allen et al., 2005, 2007), Equation (1). Consequently, the instantaneous ET ( $ET_{inst}$ ) for each pixel was calculated.

$$LE = R_n - G - H \quad (1)$$

The first step in the METRIC model was to compute the net radiation ( $R_n$ ) using the surface radiation balance, Equation (2). The  $R_n$  estimation was accomplished in a series of steps by summing up the net short-wave radiation and net long-wave radiation (Hippis, 1989; Brunsell and Gillies, 2002; Allen et al., 2007).



$$R_n = R_{s\downarrow} - \alpha R_{s\downarrow} - R_{L\downarrow} - R_{L\uparrow} - (1 - \varepsilon_o) R_{L\downarrow} \quad (2)$$

Where,  $R_{s\downarrow}$  is the incoming shortwave radiation ( $W m^{-2}$ ),  $\alpha$  is the broadband surface albedo (dimensionless),  $R_{L\downarrow}$  and  $R_{L\uparrow}$  are the inbound and outgoing longwave radiation ( $W m^{-2}$ ), respectively.  $\varepsilon_o$  is the broad-band surface thermal emissivity (dimensionless), The  $(1-\varepsilon_o) R_{L\downarrow}$  term represents the fraction of incoming longwave radiation reflected from the surface. Spectral reflectance of bands 1-7 was used to calculate surface albedo ( $\alpha$ ) as described in Allen et al. (2007).

The surface emissivity correction was performed using an empirical Equation (3) by Tasumi (2003) based on soil and vegetative thermal emissivities. Leaf area index (LAI) is computed as per Equation (4) as proposed by Bastiaanssen (1998). During the correction, the typical bare soil and the fully vegetated surface values were set as 0.93 and 0.98, respectively. where, the soil adjusted vegetation index, SAVI was calculated based on TOA reflectance of bands 4 and 5 (Huete, 1988). Subsequently, surface temperature ( $T_s$ ) was computed by converting the TIRS band data from spectral radiance to brightness temperature using the provided thermal constants in the metadata file of Landsat-8 images (USGS).

$$\varepsilon_o = 0.95 + 0.01 LAI \text{ for } LAI \leq 3 \quad (3)$$

15

$$LAI = \frac{-\ln[(0.69 - SAVI)/0.59]}{0.91} \quad (4)$$

For the estimation of soil heat flux ( $G$ ), various empirical equations can be found in the literature (Bastiaanssen, 1998; Singh et al., 2008; Gowda et al., 2011). However, this study adopted the empirical model described by Bastiaanssen (2000) representing values near midday for the prediction of Landsat-8  $G$  (i.e.  $G_{METRIC}$ ), as a ratio  $G/R_n$  based on the NDVI, Equation (5).

$$\frac{G}{R_n} = (T_s - 273.15)(0.0038 + 0.0074 \alpha)(1 - 0.98 NDVI^4) \quad (5)$$

25 Where  $T_s$  is the surface temperature (K), and  $\alpha$  is the surface albedo. Subsequently, the  $G_{METRIC}$  was obtained by multiplying  $G/R_n$  with  $R_n$ .

The sensible heat ( $H_{METRIC}$ ), however, was estimated from an aerodynamic function as expressed in Equation (6). In the calculation of  $r_{ah}$ , wind speed measurements were used.

$$30 \quad H = \rho_{air} C_p \frac{\Delta T}{r_{ah}} \quad (6)$$



Where  $\rho$  is the air density ( $\text{kg m}^{-3}$ ),  $C_p$  is the specific heat capacity of the air ( $\text{J kg}^{-1} \text{ }^\circ\text{K}^{-1}$ ),  $\Delta T$  is the near surface air temperature and  $r_{ah}$  is the aerodynamic resistance for heat transfer ( $\text{s m}^{-1}$ ) between two near-surface heights (i.e. at alfalfa canopy height and the EC measurement height). For further detail steps of  $H_{\text{METRIC}}$  computation refer Allen et al. (2007).

## 5 2.5 Calculation of ET

Following the establishment of  $R_n$ ,  $G$  and  $H$  from the Landsat-8 processing,  $LE$  was calculated as a residual of the energy balance equation. The obtained  $LE$  is equivalent to the  $ET_{\text{inst}}$  at the time of Landsat-8 overpass, (Equation (7)).

$$ET_{\text{inst}} = 3,600 \frac{LE}{\lambda \rho_w} \quad (7)$$

10

Where  $ET_{\text{inst}}$  is the instantaneous ET ( $\text{mm h}^{-1}$ ); 3,600 converts from seconds to hours,  $\rho_w$  is the density of water ( $\sim 1,000 \text{ kg m}^{-3}$ ) and  $\lambda$  is latent heat of vaporization ( $\text{J kg}^{-1}$ ) representing the heat absorbed when a kilogram of water evaporates. The  $\lambda$  component was computed as per Equation (8).

$$15 \quad \lambda = [2.501 - 0.00236 (T_s - 273.15)] \times 10^6 \quad (8)$$

Finally, as presented in Equation (9), the reference ET fraction ( $ET_{rF}$ ) was calculated as the ratio of the computed  $ET_{\text{inst}}$  from each pixel to the reference ET ( $ET_r$ ), which was computed from the weather data.

$$20 \quad ET_{rF} = \frac{ET_{\text{inst}}}{ET_r} \quad (9)$$

Where  $ET_{\text{inst}}$  is from Equation (7) and  $ET_r$  is for the standardized 0.5 m tall alfalfa at the time of the image. The EC system recorded weather parameters were used to calculate  $ET_r$  as described in ASCE-EWRI (2005). The obtained  $ET_{rF}$  was subsequently extrapolated to daily values. In the processes,  $ET_{24}$  was computed by assuming that the instantaneous  $ET_{rF}$  computed at satellite overpass is the same as the average  $ET_{rF}$  over the 24 h average (Allen et al., 2007), Equation (10).

25

$$ET_{24} = C_{\text{rad}} (EF)(ET_{r24}) \quad (10)$$

Where  $ET_{24}$  is the cumulative ET ( $\text{mm day}^{-1}$ ) for the day of the image overpass;  $C_{\text{rad}}$  is the correction term used in sloping terrain to correct for variation in 24 h versus instantaneous energy availability.  $ET_{rF}$  is from Equation (9) and  $ET_{r24}$  is the cumulative reference ET for the day of the image (Van Niel et al., 2012; Cammalleri et al., 2014).

30



## 2.6 Data analysis

The spatially estimated energy flux components, derived from the METRIC algorithm and the EC flux tower, were subjected to heat flux correction and energy balance and footprint (FTP) analysis, as described in Schmid (1994), Twine et al. (2000) and Kustas et al. (2005). In the FTP analysis, the utilized wind parameters such as wind speed, wind direction and yaw angle  
5 at the time of Landsat-8 overpass were provided in **Table 2**. On the other hand, different statistical performance indicators (RMSE, MBE and Nash-Sutcliff coefficient) were utilized for the assessment of the METRIC performance in estimating ET against the EC system.

## 3 Results and discussion

### 2.3 Footprint analysis (FTP)

10 The simple arithmetic averages of weighted/integrated heat fluxes over the fetch areas are the FTPs (Chavez et al., 2005). FTPs are widely used in validating the spatially distributed fluxes obtained from remote sensing (RS) with EC measured fluxes. The fetch area of the FTP was classified into six classes, based on the cumulative contribution of the eddies, as provided in **Figure 2**. Based on the FTP analysis, about 90% of the EC system observed eddies originated from the 122 to 144 m in the upwind direction. However, the peak (vertical) fetch was within 42 to 51 m. It was also observed that 10% of  
15 the fluxes were registered between 6 and 17.5 m from the flux tower. Whereas, about 30%, 50% and 70% of the fluxes were recorded between 35 to 63 m, 52 to 97 m and 81 to 136 m, respectively. On the other hand, energy fluxes were analyzed as per Chavez et al. (2005) by integrating Landsat-8 image acquisition (i.e. overpass), which showed the 90% of the FTP overlap with METRIC model (Kustas et al., 2005). Hence, the obtained leaf area index ( $LAI_G$ ) and the reference ET ( $ET_r$ ) over the alfalfa field were used as inputs to the METRIC-based Landsat-8 ET prediction (**Table 3**). The ground-based LAI  
20 ( $LAI_G$ ) of alfalfa was recorded on the day of satellite overpass using plant canopy analyzer (LAI-2200).

### 3.1 Surface temperature (T)

As illustrated in **Figure 3**, linear regression analysis of Landsat-8 derived surface temperature ( $T_{LST}$ ) using the METRIC algorithm against the EC flux tower measured temperature ( $T_{EC}$ ) showed a good correlation with an  $R^2$  value of 0.71 ( $P = 0.0084$ ). However, the METRIC algorithm was observed to underestimate the  $T_{LST}$  compared to the  $T_{EC}$  as evidenced by the  
25 RMSE and MBE performance indicators of  $4.23^\circ\text{C}$  (-12.82 %) and  $-3.40^\circ\text{C}$  (-9.34%), respectively. The recorded errors (4.2 % to 19.6%) in the METRIC estimated surface temperature were slightly higher than the values reported in previous studies. For example, compared to lysimeters, Chavez et al. (2009a) reported METRIC errors of 11.1% and 1.9% in estimating surface temperatures for corn and sorghum fields, respectively. According to Omran (2012), LAI affected the amount of heat stored in the soil surface through transpiration process, and this was evident with the Landsat-8 derived  $T_{LST}$  with an error of  
30 about 20%, where the alfalfa crop was in full foliage cover (i.e. LAI=6). Thus, the temporal variation in LAI would result in



oscillations of the land surface temperature. As an example, at a low LAI (<1.23) during the Day Of the Year (DOY) of 154, 234 and 266, high  $T_{LST}$  (> 34.3 °C) values were recorded in the experimental alfalfa field. However, there is a discrepancy at higher temperatures when the crop density of alfalfa was low (i.e. bare soil was visible to the radiometer) as evidenced by the low LAI values over the footprint and the recorded  $T_{EC}$  and  $T_{LST}$  (Chavez et al., 2005). Hence, the cooling effect of  
5 vegetation on the  $T_{LST}$  accelerated the error by 1 to 20% during the low and high LAI cases, respectively.

### 3.2 Energy balance (EB) components

The mean values of energy balance (EB) components obtained from both the EC system and METRIC algorithm are provided in **Table 4**. While, the performance indicators (RMSE, MBE and Nash-Sutcliff coefficient) are given in **Table 5**.

#### 3.2.1 Net radiation ( $R_n$ )

10 The temporal trend of EC (CNR-4) measured  $R_n$  ( $R_{nEC}$ ) was analyzed for discrepancies. About 9% to 16% of the collected data exhibited infrequent errors; and hence, the abnormal data has been discarded, and a gap-filling process was performed using the Eddy Pro software program (version 5.0). A scatter plot (Figure 4), representing the relationship between  $R_{nEC}$  and METRIC estimated  $R_n$  ( $R_{nRS}$ ), was generated and analyzed for performance accuracy. Moderate linear correlation ( $R^2 = 0.54$  and  $P>F = 0.0381$ ), low RMSE (18.32 W m<sup>-2</sup>; 3.8%) and very low MBE (8.66 W m<sup>-2</sup>; 1.76%) indicated that the METRIC  
15 model accurately (96%) estimated the  $R_n$ . The obtained RMSE and MBE values are in agreement with those reported by earlier studies of Mkhwanazi and Chavez (2012) where the RMSE value was 4.1% and MBE value was 3.3%, and Chavez et al. (2007) where the RMSE value was 9.8% for METRIC model estimated  $R_n$  using Landsat-8 TM image.

#### 3.2.2 Soil heat flux (G)

**Figure 5** illustrates a scatter plot between the EC measured ( $G_{EC}$ ) and the METRIC estimated ( $G_{RS}$ ) soil heat flux values.  
20 The relationship was relatively fair with an  $R^2$  value of 0.67 and a Nash-Sutcliffe coefficient of 0.59. The RMSE and MBE, however, were determined at 28.46 W m<sup>-2</sup> (37.33%) and 12.42 W m<sup>-2</sup> (16.29%), respectively. These recorded errors were relatively higher than the values reported in similar previous studies. Mkhwanazi and Chavez (2012) reported an RMSE value of 14.2 W m<sup>-2</sup> (27.6%) and an MBE value of -3.0 W m<sup>-2</sup> (-5.8%) in estimating G with the METRIC algorithm for irrigated alfalfa. The average observed values of G were similar to the majority of values recorded by Ham et al. (1991).  
25 Furthermore, the ratio of  $R_n$  to the G ( $G/R_n$ ) derived from METRIC model against the LAI inferred from the Canopy analyser (PCA 2200, Li-COR, USA) is presented in **Figure 6**. The  $G/R_n$  is one of the essential components in the analysis of the accuracy of Bowen ratio (Allen et al., 2011b). Correlating the LAI with the  $G/R_n$  produced a moderate polynomial (3<sup>rd</sup> order) relationship for both the METRIC ( $R^2 = 0.288$  and  $P>F = 0.23$ ) and the EC ( $R^2 = 0.313$  and  $P>F = 0.15$ ) methods. However, the results suggested that beyond a certain value of LAI (up to 4.2), the relationship between the  $G/R_n$  and LAI  
30 was constant. The scatter in the  $G/R_n$  where the values for LAI > 4 is not surprising since the values of  $G/R_n$  for full canopy cover are ranging between 0.05 and 0.15 as showed in Waters et al. (2002).





### 3.2.3 Sensible heat flux (H)

Comparison between the METRIC estimated H ( $H_{RS}$ ) and the EC measured H ( $H_{EC}$ ), after the adjustments of EB closure, showed values of mean estimation error ranging from  $10.89 \text{ W m}^{-2}$  (low LAI conditions) to  $38.91 \text{ W m}^{-2}$  (full canopy condition) with an MBE value of  $15.72 \text{ W m}^{-2}$  (13.87%). The high RMSE value of  $72.01 \text{ W m}^{-2}$  (63.54%) for the  $H_{RS}$  might be due to the advection and variability in the canopy density. Hence, most of the  $R_n$  has been partitioned into LE than into H, as introduced by the near surface air temperature difference ( $\Delta T$ ) and the aerodynamic resistance of heat transfer ( $r_{ah}$ ), i.e. propagation errors. This was evident in the linear regression analysis (**Figure 7**), where a good correlation between the  $H_{RS}$  and  $H_{EC}$  ( $R^2 = 0.61$ ) was observed; however, it was not significant ( $P > F = 0.022$ ), and it was also confirmed with the RMSE of 63.5%. In contrast, Carrasco-Benavides et al. (2013) reported that the METRIC algorithm overestimated the H component by  $39 \text{ W m}^{-2}$  with a mean absolute error of 10%.

### 3.2.4 Latent heat flux (LE)

A scatter plot was established between the METRIC estimated ( $LE_{RS}$ ) and the EC determined LE ( $LE_{EC}$ ) values as illustrated in **Figure 8**. The correlation was relatively good ( $R^2 = 0.66$ ); however, it was not statistically significant ( $P > F = 0.14$ ). This was attributed to the fact that the  $LE_{RS}$  was a residual component of the energy balance equation that mainly depends on the calibration accuracy of the  $H_{RS}$ , which was purely based on the quality of the selected anchor pixels (Weaver, 1990; Field et al., 1994).

Although the regression analysis showed a non-significant correlation, the performance indicators such as the MBE ( $2.45 \text{ W m}^{-2}$ ; 0.73%) and the RMSE ( $115.04 \text{ W m}^{-2}$ ; 34.33%) are in accordance with the earlier reported values indicating that the METRIC algorithm was useful in the accurate determination of LE over large areas. However, Carrasco-Benavides et al. (2013) stated that the METRIC algorithm overestimated the LE by 14% (RMSE). The obtained average absolute error of the  $LE_{RS}$  for the eight images was 35%. **Figure 9** illustrates the Energy Balance (EB) components, where the LE and the G are presented as the major and the minor EB components, respectively.

### 3.2.5 Evapotranspiration (ET)

The correlation between the ET values obtained from both the METRIC algorithm and the EC system was found to be highly significant ( $R^2 = 0.93$  and  $P > F = 0.0001$ ) as illustrated in **Figure 10**. Further assessment of the accuracy of the METRIC algorithm in estimating the ET was performed using the RMSE and MBE indicators. Comparing the hourly ET calculated using the METRIC algorithm to that using the EC system resulted in an RMSE value of  $0.09 \text{ mm h}^{-1}$  (14.33%) and an MBE value of  $0.04 \text{ mm h}^{-1}$  (6.46%). For the daily mean ET, the RMSE and MBE values were  $2.25 \text{ mm d}^{-1}$  (25.93%) and  $0.38 \text{ mm d}^{-1}$  (4.40%), respectively. These results are in agreement with the results reported by Mkhwanazi and Chavez (2012), where the performance errors in estimating the ET using the METRIC model were determined at  $0.14 \text{ mm h}^{-1}$  (17.6%) and  $-0.08$



mm h<sup>-1</sup> (-10.3%) for RMSE and MBE, respectively. Similarly, Chavez et al. (2007) reported a METRIC error of 0.7 mm d<sup>-1</sup> (7.4 %) in predicting the ET compared to lysimeter data.

### 3.2.6 Energy balance (EB)

5 Eddy Covariance (EC) system facilitates the process of accurate measurements of energy balance (EB) components. Hence, using the measured EB components, the surface energy budget can be estimated (Equation 1) along with the EB closure. The four flux components ( $R_n$ ,  $H$ ,  $G$  and  $LE$ ) measured by the EC system were assessed for the EB closure (Kustas et al., 2005). The EB closure rate for the EC system ranged between 71% and 99%, with a mean value of 87% (**Table 6**). Energy balance  
10 equation due to advection and measurement errors in the field) in the partition of the net radiation into latent and sensible heat fluxes and soil heat flux. This was attributed to the inherent errors in measuring the EB components by the ground systems, which was reported to be 15 - 20%, 5 - 10% and 20 - 30% according to Weaver (1990), Field et al. (1994) and Twine et al. (2000), respectively.

## 15 4 Conclusions

The METRIC algorithm was applied on Landsat-8 images for the ET mapping, and its performance was evaluated against the EC flux tower measured EB components and ET at hourly and daily intervals over irrigated alfalfa field in the Eastern Region of Saudi Arabia. The following are the specific conclusions of this study:

- 20 • The METRIC algorithm was successfully utilized to estimate the ET with an average error of 6.6% (hourly ET) and 4.2% (daily ET). The performance of the METRIC algorithm was found to be more accurate in estimating the hourly ET ( $R^2 = 0.93$ ) than the daily ET ( $R^2 = 0.57$ ) compared to the  $ET_{EC}$ .
- 25 • Due to the cooling effect of vegetation, it was found that the METRIC algorithm underestimated the surface temperature ( $T_{LST}$ ) by 1% and 20% for partial and full canopy conditions, respectively. However, the METRIC algorithm produced accurate LE estimates which were indicated by the low mean value of MBE of 2.45 W m<sup>-2</sup> (0.74%).
- Compared with the EC data, the RS estimated  $R_n$  component was found to be highly accurate (an accuracy of more than 95%). In addition, the sensible heat flux obtained from satellite data was associated with errors ranging between 10.89 W m<sup>-2</sup> and 38.91 W m<sup>-2</sup> at low (< 1.2) and high (>5.0) LAI values, respectively.



## Acknowledgements

The authors are grateful to the Deanship of Scientific Research, King Saud University for funding through the Vice Deanship of Scientific Research Chairs. The unstinted cooperation and support extended by Mr. Alan King and Mr. Jack King in carrying out the field research work are gratefully acknowledged. The guidance provided by the subject experts:

- 5 Biradar, C.M., ICARDA, Jordan and Gowda, P. H., USDA during the study and preparation of the manuscript was quite valuable.

## References

- Al-Ghobari, H. M., Mohammad, F. S. and ElMarazky, M. S. A.: Effect of intelligent irrigation on water use efficiency of wheat crop in arid region, *J. Anim. Plant Sci.*, 23, 1691-1699, 2013.
- 10 Al-Kahtani, S. H. and Ismaiel, S. M.: Groundwater irrigation management in the Kingdom of Saudi Arabia: A case study of Al-Wajid aquifer, *J. US-China Public Admin.*, 7, 54-65, 2010.
  - Allen, R. G., Pereira, S. L., Howell, T. A. and Jensen, M. E.: Evapotranspiration information reporting: I. Factors governing measurement accuracy, *Agr. Water Manage.*, 98, 899-920, doi: 10.1016/j.agwat.2010.12.015, 2011a.
  - Allen, R., Irmark, A., Trezza, R., Hendrickx, J. M. H.: Bastiaanssen, W. G. M., Kjaersgaard, J.: Satellite based ET estimation in agriculture using SEBAL and METRIC, *Hydrol. Process.*, 25, 4011-4027, doi: 10.1002/hyp.8408, 2011b.
  - 15 Allen, R. G., Tasumi, M., Morse, A. and Trezza, R.: A Landsat-based energy balance and evapotranspiration model in Western US water rights regulation and planning, *Irrig. Drain. Syst.*, 19, 251-268, doi:10.1007/s10795-005-5187-z, 2005.
  - Allen, R. G., Tasumi, M., Morse, A., Trezza, R., Wright, J. L., Bastiaanssen, W., Kramber, W., Lorite, I. and Robinson, C. W.: Satellite-Based Energy Balance for Mapping Evapotranspiration with Internalized Calibration (METRIC)—Applications, *J. Irrig. Drain. Eng.*, 133, 395-406, 2007.
  - 20 Anderson, M. C., Allen, R. G., Morse, A. and Kustas, W. P.: Use of Landsat thermal imagery in monitoring evapotranspiration and managing water resources, *Remote Sens. Environ.*, 122, 50-65, doi: 10.1016/j.rse.2011.08.025, 2012.
  - 25 ASCE-EWRI: Final report-2005, The ASCE standardized reference evapotranspiration equation, <https://www.kimberly.uidaho.edu/water/asceewri/ascestzdetmain2005.pdf>, 2005
  - Atta, R., Boutraa, T. and Akhkha, A.: Smart Irrigation System for Wheat in Saudi Arabia Using Wireless Sensors Network Technology, *Int. J. Water Resour. Arid Environ.*, 1, 478-482, 2011.
  - Bala, A., Singh, R. K. and Gayathri, V.: Review on different Surface Energy Balance algorithms for Estimation of Evapotranspiration through Remote Sensing, *Int. J. Emerging Technol. Adv. Engineer.*, 3, 582-588, 2013.
  - 30 Bastiaanssen, W. G. M., Menenti, M., Feddes, R. A. and Holtslag, A. A. M.: A Remote sensing surface energy balance algorithm for land (SEBAL): 1. Formulation,” *Journal of Hydrology*, vol. 212-213, pp. 198-212, 1998.



- Bastiaanssen, W. G. M., Molden, D. J. and Makin, I. W.: Remote sensing for irrigated agriculture: examples from research and possible applications, *Agr. Water Manage.*, 46, 137-155, doi: 10.1016/S0378-3774(00)00080-9, 2000.
- Brunsell, N. A. and Gillies, R.: Incorporating surface emissivity into a thermal atmospheric correction, *Photogramm. Engineer. Remote Sens. J.*, 68, 1263-1269, 2002.
- 5 Cammalleri, C., Anderson, M. C. and Kustas, W. P.: Upscaling of evapotranspiration fluxes from instantaneous to daytime scales for thermal remote sensing applications, *Hydrol. Earth Syst. Sci.*, 18, 1885–1894, 2014.
- Carrasco-Benavides, M., Ortega-Farias, S., Lagos, L. O. and Kleissl, J.: Assessment of the METRIC model in the estimation of instantaneous values of sensible and latent heat fluxes over a drip-irrigated Merlot vineyard using Landsat images, in the Proceedings of the Anais XVI Simposio Brasileiro de Sensoriamento Remoto - SBSR, Foz do Iguaçu, PR, Brasil,
- 10 13-18 April 2013, pp. 490-497, 2013.
- Chavez, J. L., Gowda, P. H., Howell, T. A. and Copeland, K. S.: Evaluating three evapotranspiration mapping algorithms with lysimetric data in the semi-arid Texas High Plains,” in the Proceedings of the 28<sup>th</sup> Annual International Irrigation Show. Irrigation Association, 9-11 December 2007, San Diego, California, USA. Pp. 268-283, 2007.
- Chavez, J. L., Gowda, P. H., Howell, T. A. and Copeland, K. S.: Radiometric surface temperature calibration effects on
- 15 satellite based evapotranspiration estimation, *Int. J. Remote Sens.*, 30, 2337-2354, 2009a.
- Chavez, J. L., Howell, T. A. and Copeland, K. S.: Evaluating eddy covariance cotton ET measurements in an advective environment with large weighing lysimeters, *Irrig. Sci.*, 28, 35-50, 2009b.
- Chavez, J. L., Neale, C. M. U., Hippias, L. E., Prueger, J. H. and Kustas, W. P.: Comparing Aircraft-Based Remotely Sensed Energy Balance Fluxes with Eddy Covariance Tower Data Using Heat Flux Source Area Functions, *J. Hydrometeorol.*,
- 20 6, 923-940, doi: 10.1175/JHM467.1, 2005.
- Colaizzi, P. D., Evett, S. R., Howell, T. A. and Tolk, J. A.: Comparison of Five Models to Scale Daily Evapotranspiration from One-Time-of-Day Measurements, *Trans. Amer. Soc. Agric. Biol. Engineer*, 49, 1409-1417, 2006.
- Ding, R., Kang, S., Li, F., Zhang, Y., Tong, L. and Sun, Q.: Evaluating eddy covariance method by large-scale weighing lysimeter in a maize field of northwest China, *Agric. Water Manage.*, 98, 87-95, 2010.
- 25 Drexler, J. Z., Snyder, R. L., Spano, D. and Paw, U. K. T.: A review of models and micrometeorological methods used to estimate wetland evapotranspiration, *Hydrol. Process.*, 18, 2071-2101, 2004.
- Elnesr, M. and Alazba, A.: Effect of climate change on spatiotemporal variability and trends of evapotranspiration, and its impact on water resources management in the Kingdom of Saudi Arabia, in: B. R. Singh, (Ed.): *Climate Change – Realities, Impacts over Ice Cap, Sea Level and Risks*, InTech, Rijeka, Croatia, 273-296, 2013.
- 30 FAO.: Guidelines for predicting crop water requirements, in Doorenbos, J. and Pruitt, W. O. (eds.), *FAO Irrigation and Drainage Paper. Paper No. 24*, p. 144. Food and Agriculture Organization of the United Nations, Rome. 1977. <http://www.fao.org/docrep/018/f2430e/f2430e.pdf>, 1977.
- Farah, H. O., Bastiaanssen, W. G. M. and Feddes, R. A.: Evaluation of the temporal variability of the evaporative fraction in a tropical watershed, *Int. J. Appl. Earth Observe. Geoinf.*, 5, 129-140, 2004.



- Field, R. T. Heiser, M. and Strebel, D. E.: Measurements of surface fluxes, in the FIFE Information System, Summary Document, [http://www.esm.versar.com/FIFE/Summary/Sur\\_flux.htm](http://www.esm.versar.com/FIFE/Summary/Sur_flux.htm), 1994.
- Gowda, P. H., Chavez, J. L., Howell, T. A., Marek, T. H. and New, L. L.: Surface Energy Balance Based Evapotranspiration Mapping in the Texas High Plains, *Sensors*, 8, 5186-5201, 2008.
- 5 Gowda, P. H., Howell, T. A., Paul, G. and Colaizzi, P. D.: SEBAL for estimating hourly ET fluxes over irrigated and dryland cotton during BEAREX08, in the Proceedings of the World Environmental and Water Resources Congress-2011, May 22-26, 2011, Palm Springs, California, USA; pp. 2787-95, 2011.
- Gowda, P. H., Howell, T. A., Paul, G., Colaizzi, P. D., Marek, T. H., Su, B. and Copeland, K. S.: Deriving Hourly Evapotranspiration Rates with SEBS: A Lysimetric Evaluation, *Vadose Zone J.*, 12, 1-11, doi: 10.2136/vzj2012.0110,  
10 2013.
- Hipps, L. E.: The infrared emissivities of soil and *Artemisia tridentate* and subsequent temperature corrections in a shrubsteppe ecosystem, *Remote Sens. Environ.*, 27, 337-342, 1989.
- Hoedjes, J. C. B., Chehbouni, A., Jacob, F., Ezzahar, J. and Boulet, G.: Deriving daily evapotranspiration from remotely sensed instantaneous evaporative fraction over olive orchard in semi-arid Morocco, *J. Hydrol.*, 354, 53-64, doi:  
15 10.1016/j.jhydrol.2008.02.016, 2008.
- Huete, A.R.: A soil-adjusted vegetation index (SAVI), *Remote Sens. Environ.*, 25, 295-309, doi: 10.1016/0034-4257(88)90106-X, 1988.
- Hussain, G., Alquwaizany, A. and Al-Zarah, A.: Guidelines for irrigation water quality and water management in the Kingdom of Saudi Arabia – an overview, *J. Appl. Sci.*, 10, 79-96, 10.3923/jas.2010.79.96, 2010.
- 20 Kalma, J. D., McVicar, T. R. and McCabe, M. F.: Estimating land surface evaporation: a review of methods using remotely sensed surface temperature data, *Surv. Geophys.*, 29, 421-469, 2008.
- Kassem, M. A. and Al-Moshileh, A. M.: Determination of the Best of Irrigation System for Water Conservation, in: The 3<sup>rd</sup> International Conference on Water Resources and Arid Environments (ICWRAE) and the 1<sup>st</sup> Arab Water Forum, Riyadh, Saudi Arabia, 16-19, November, 2008. <http://www.icwrae-psipw.org/images/stories/2008/Water/61.pdf>
- 25 Kustas, W. P., Hatfield, J. L. and Prueger, J. H.: The Soil Moisture–Atmosphere Coupling Experiment (SMACEX): Background, hydrometeorological conditions, and preliminary findings, *J. Hydrometeorol*, 6, 791-804, 2005.
- Lagos, L. O., Lillo-Saavedra, M., Fonseca, D. and Gonzalo, C.: Evapotranspiration of partially vegetated surfaces from remote sensing, in: Lasaponara, R., Masini, N. and Biscione, M. (Eds.): Towards Horizon 2020, the Proc. 33<sup>rd</sup> EARSeL Symposium, 3-6 June, 2013, Matera, Italy; pp. 613-624, 2013.
- 30 LI-COR.: Eddypro Instruction Manual,” LI-COR Biosciences, Lincoln, Nebraska, USA, pp: 332. <https://www.licor.com/documents/1ium2zmwm6hl36yz9bu4>
- Mkhwanazi, M. M. and Chavez, J. L.: Using METRIC to Estimate Surface Energy Fluxes over an Alfalfa Field in Eastern Colorado, *Hydrology Days 2012*, 90-98, [http://hydrologydays.colostate.edu/Papers\\_2012/Mcebisi\\_paper.pdf](http://hydrologydays.colostate.edu/Papers_2012/Mcebisi_paper.pdf), 2012.



- Mohammad, F. S., Al-Ghobari, H. M. and ElMarazky, M. S. A.: Adoption of an intelligent irrigation scheduling technique and its effect on water use efficiency for tomato crops in arid regions, *Aust. J. Crop Sci.*, 7, 305-313, doi:10.1002/ird.518, 2013.
- Moorhead, J. E., Gowda, P. H., Marek, T. H., Porter, D. O., Howell, T. A., Singh, V. P. and Stewart, B. A.: Use of crop-specific drought indices for determining irrigation demand in the Texas High Plains, *Appl. Eng. Agr.*, 26, 905-916, doi: 10.13031/aea.29.10201, 2013.
- 5 Omran, EL. E.: Detection of land-use and surface temperature change at different resolutions, *J. Geograph. Inf. Sys.*, 4, 189-203, 2012.
- Patil, V. C., Al-Gaadi, K. A., Madugundu, R., Tola, E., Marey, S., Aldosari, A., Biradar, C. M. and Gowda, P. H.: Assessing Agricultural Water Productivity in Desert Farming System of Saudi Arabia,” *IEEE J. Sel. Top. Appl. Earth Observe. Remote Sens.*, 8, 284-297, 2015.
- 10 Paul, G., Gowda, P. H., Prasad, P. V. V., Howell, T. A., Staggenborg, S. A. and Neale, C. M. U.: Lysimetric evaluation of SEBAL using high resolution airborne imagery from BEAREX08, *Adv. Water Resour.*, 59, 157-168, 2013.
- Praveen, P., Vivek, S. D., Desai, G. A., Praveen, G. S. and Meerabai, K. P.: Estimation of evapotranspiration rate by different methods for paddy crop in South Kodagu, Central Western Ghats, *Int. J. Agr. Eng.*, 5, 69-72, 2012.
- 15 Rana, G. and Katerji, N.: Measurement and estimation of actual evapotranspiration in the field under Mediterranean climate: a review, *Eur. J. Agron.*, 13, 125-153, doi: 10.1016/S1161-0301(00)00070-8, 2000.
- Rizaiza, O. S. A. and Al-Osaimy, M. H.: A statistical approach for estimating irrigation water usage in western Saudi Arabia, *Agr. Water Manage.*, 29, 175-185, doi:10.1016/0378-3774(95)01194-3, 1996.
- 20 Santos, C. A. C., Silva, B. B. and Rao, T. V. R.: Analyses of the evaporative fraction using eddy covariance and remote sensing techniques, *Revista Brasileira de Meteorologia*, 25, 427-436, doi: 10.1590/S0102-77862010000400002, 2010.
- Schmid, H. P.: Source areas for scalars and scalar fluxes, *Bound-Layer Meteorol.*, 67, 293-318, 1994.
- Senay, G. B., Verdin, J. P., Lietzow, R. and Melesse, A. M.: Global Daily Reference Evapotranspiration Modeling and Evaluation, *J. Amer. Water Resour. Assoc.*, 44, 969-979, doi: 10.1111/j.1752-1688.2008.00195.x, 2008.
- 25 Singh, R. K., Irmak, A., Irmak, S. and Martin, D. L.: Application of SEBAL Model for mapping evapotranspiration and estimating surface energy fluxes in South-Central Nebraska, *J. Irrig. Drain. Eng.*, 134, 273-285, 2008.
- Twine, T. E., Kustas, W. P., Norman, J. M., Cook, D. R. and Houser, P. R.: Correcting eddy-covariance flux underestimates over a grassland, *Agric. For. Meteorol.*, 103, 279-300, 2000.
- USGS, Using the USGS Landsat 8 Product. <https://landsat.usgs.gov/using-usgs-landsat-8-product>
- 30 Van Niel, T. G., McVicar, T. R., Roderick, M. L., Van Dijk, A. I. J. M., Beringer, J. S., Hutley, L. B. and Van Gorsel, E.: Upscaling latent heat flux for thermal remote sensing studies: Comparison of alternative approaches and correction of bias, *J. Hydrol.*, 468-469, 2012.
- Waters, R., Allen, R. G., Tasumi, M., Trezza, R. and Bastiaanssen, W.: SEBAL—Advanced Training and User’s Manual, Version 1 (from NASA EOSDIS/Synergy grant from the Raytheon Company, through The Idaho Department of Water



- Resources, USA), Kimberly, ID, USA: University of Idaho, 98p, 2002. <http://www.posmet.ufv.br/wp-content/uploads/2016/09/MET-479-Waters-et-al-SEBAL.pdf>.
- Weaver, H. L.: Temperature and humidity flux-variance relations determined by one-dimensional eddy correlation, Bound-Layer Meteorol., 53, 77-91, 1990.
- 5 Yee, M. S., Beringer, J., Pauwels, V. R. N., Daly, E., Walker, J. P. and Rudiger, C.: Measuring evapotranspiration: comparison of eddy covariance, scintillometers and enclosed chambers, Geophysical Research Abstracts, EGU2014-4590, EGU General Assembly 2014. <http://meetingorganizer.copernicus.org/EGU2014/EGU2014-4590.pdf>, 2014
- Zeweldi, D. A., Gebremichael, M., Wang, J., Sammis, T., Kleissl, J. and Miller, D.: Intercomparison of Sensible Heat Flux from Large Aperture Scintillometer and Eddy Covariance Methods: Field Experiment over a Homogeneous Semi-arid Region, Bound.-Layer Meteorol., 135, 151-159, doi: doi:10.1007/s10546-009-9460-9, 2010.
- 10



## Tables

**Table 1.** Details of Landsat-8 data used in the study.

Path	Row	Date of overpass
165	43	June 3, June 19, July 5, July 21, August 22, September 7, September 23 and October 9, 2013

5

**Table 2.** Details of wind parameters at the time of satellite overpass

Date	Wind Speed (m/s)		Wind Direction (° from North)	Yaw angle (°)
	Min.	Max.		
03 June, 2013	6.02	12.45	13.54	56.46
19 June, 2013	5.61	9.69	6.49	63.51
05 July, 2013	2.43	5.28	23.98	46.02
21 July, 2013	5.25	10.71	35.13	34.87
22 August, 2013	1.61	4.91	27.80	42.20
07 September, 2013	1.11	8.17	59.82	10.18
23 September, 2013	5.12	8.93	38.13	31.87
09 October, 2013	4.60	8.67	25.40	44.60

10 **Table 3.** Input parameters used for METRIC model for alfalfa crop.

DOY	$T_{EC}$ (°C)	$T_{LST}$ (°C)	$LAI_G$	$ET_r$	$u$ (m s <sup>-1</sup> )	$h_c$ (m)	$Z_m$ (m)
154	36.42	34.67	1.22	1.21	0.55	0.39	3.2
170	39.59	33.01	3.28	0.61	0.43	0.48	3.2
186	34.7	32.32	4.29	0.83	0.46	0.59	2.2
195	40.96	32.6	5.92	0.96	0.68	0.51	3.0
234	42.98	40.99	1.11	0.31	0.62	0.24	3.0
250	35.48	32.09	3.19	0.52	0.65	0.52	3.0
266	34.52	34.18	1.13	0.27	0.39	0.29	2.3
282	26.78	24.36	2.28	0.41	0.40	0.52	3.2

DOY – Day of the year;  $T_{EC}$  – Temperature from flux tower;  $T_{LST}$  – estimated temperature from Landsat-8 images;  $LAI_G$  – Ground measured Leaf Area Index;  $ET_r$  – Reference ET;  $u$  – Average horizontal wind velocity;  $h_c$  – alfalfa canopy height;  $Z_m$  – Height of wind speed measurement.





**Table 4.** EC measured and METRIC estimated Energy Balance (EB) components over an alfalfa field.

EB Component	Method	Date of Landsat-8 overpass (Day of the year 2013)							
		June 03 (154)	June 19 (170)	July 05 (186)	July 21 (195)	Aug. 22 (234)	Sept. 07 (250)	Sept. 23 (266)	Oct. 09 (282)
Soil Heat Flux (G), W m <sup>-2</sup>	RS	28.6	92.5	143.73	80.65	97.92	48.16	19.98	98.31
	ECB	21.6	44.1	155.18	70.33	37.54	54.98	16.50	110.30
Net Radiation (R <sub>n</sub> ), W m <sup>-2</sup>	RS	488.7	491.5	491.07	490.64	502.95	489.37	491.76	477.75
	ECB	468.0	500.6	506.22	463.27	513.17	476.86	469.6	456.49
G/R <sub>n</sub>	RS	0.06	0.19	0.29	0.16	0.19	0.10	0.04	0.21
	ECB	0.05	0.09	0.31	0.15	0.07	0.12	0.04	0.24
Sensible Heat Flux (H), W m <sup>-2</sup>	RS	-57.2	184.2	286.10	160.45	1.77	95.75	39.98	195.62
	EC	-65.8	112.3	274.59	127.34	14.26	230.79	19.03	68.39
Latent Heat Flux (LE), W m <sup>-2</sup>	RS	574.5	214.8	61.25	249.55	500.20	345.46	551.72	183.82
	EC	335.7	160.2	72.12	260.79	637.84	505.40	560.80	148.80
Evapotranspiration (ET), mm hr <sup>-1</sup>	RS	0.86	0.32	0.09	0.42	0.76	0.52	0.83	0.27
	EC	0.64	0.24	0.11	0.38	0.96	0.71	0.89	0.22

RS - Remote Sensing (METRIC algorithm), EC - Eddy Covariance, and ECB - Biomet sensors of Eddy Covariance system.

5

**Table 5.** Performance indicators results for the METRIC algorithm estimated EB components.

Error		G	Rn	H	LE	ET	ET
		W m <sup>-2</sup>	W m <sup>-2</sup>	W m <sup>-2</sup>	W m <sup>-2</sup>	mm hr <sup>-1</sup>	mm d <sup>-1</sup>
RMSE	Amount	28.46	18.32	72.01	115.04	0.13	4.15
	%	37.33	3.74	63.54	34.33	25.91	34.33
MBE	Amount	12.42	8.66	15.72	2.45	-0.01	0.08
	%	16.29	1.76	13.87	0.73	-1.97	0.69
Nash-Sutcliffe Coefficient		0.59	1.00	0.59	0.88	0.99	0.99
R <sup>2</sup>		0.67	0.54	0.61	0.66	0.81	0.66
P>F		0.0131	0.038	0.0216	0.0137	0.002	0.013



5 **Table 6.** Energy Balance analysis of EC measured heat fluxes.

Date (Year 2013)	Stability parameter ( $\xi$ )	Condition	Bowen Ratio	Energy Balance Closure %
3-June	0.02	Stable	-0.17	90.84
19-June	-0.15	Unstable	0.7	95.81
5-July	0.07	Neutral	-0.24	99.14
21-July	-0.24	Unstable	0.63	96.80
22-August	-0.28	Unstable	-0.42	80.82
7-September	0.04	Stable	-0.42	84.09
23-September	-0.03	Unstable	0.14	75.14
9-October	0.04	Stable	-0.13	71.74
Average	-0.06		0.01	86.79



Figures

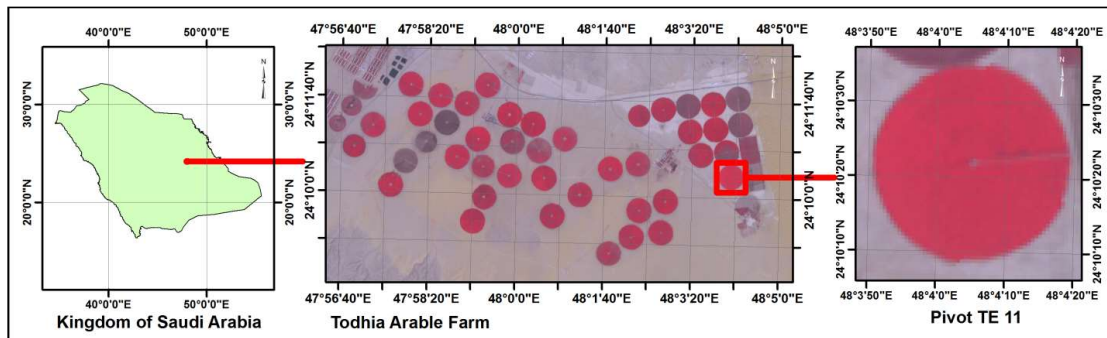


Figure 2. Location map of the study area

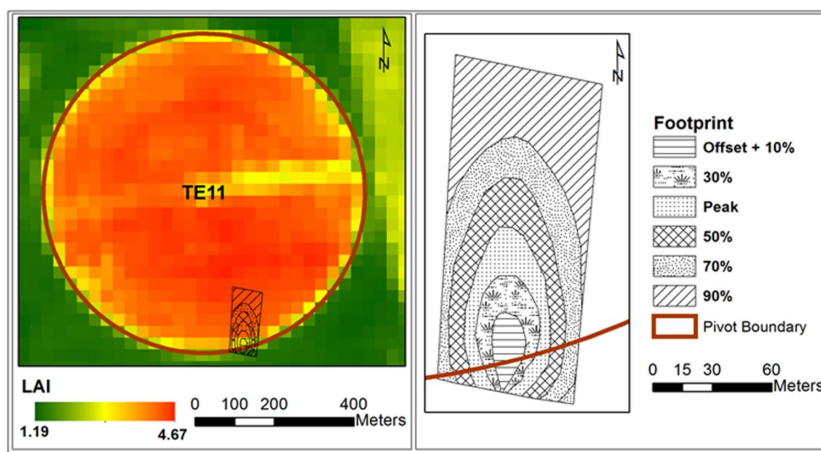
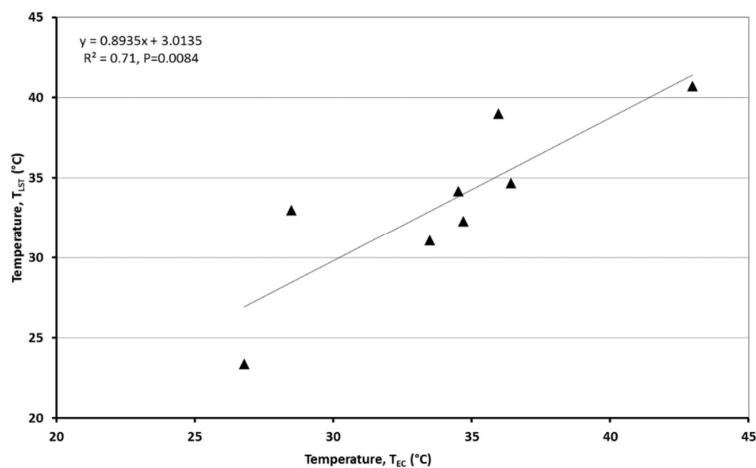
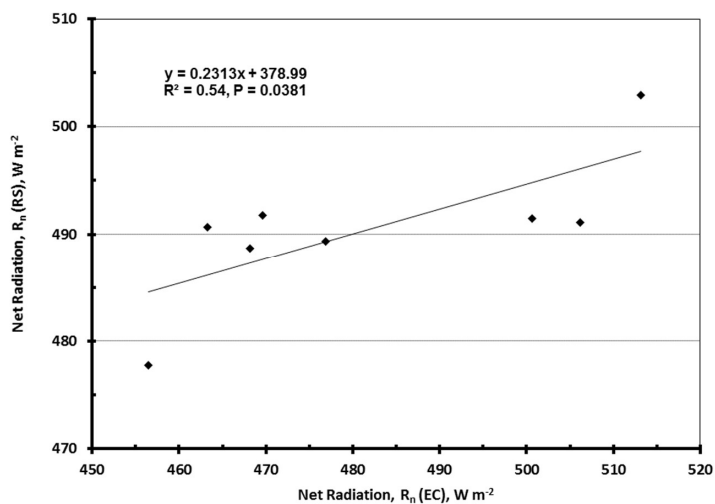


Figure 1. Flux Source Area Model (FSAM) Footprint, as % of the fetch area, of the Eddy Covariance system overlaid on LAI map of the alfalfa crop.



**Figure 3.** Comparison of EC measured ( $T_{EC}$ ) and remote sensing derived ( $T_{LST}$ ) surface temperature.

5



**Figure 4.** Comparison between the measured ( $R_{n(EC)}$ ) and METRIC derived ( $R_{n(RS)}$ ) net radiation.

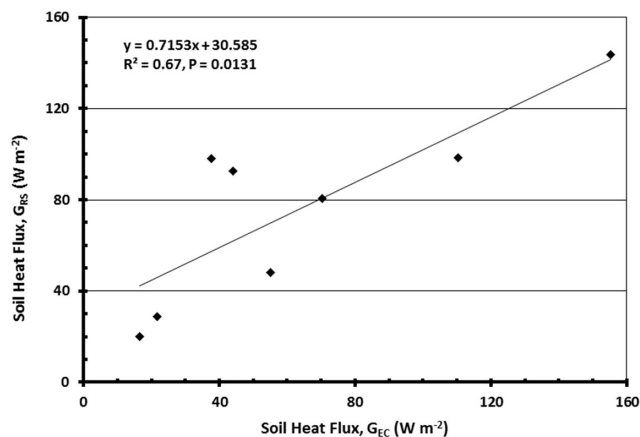


**Figure 5.** Estimated ( $G_{RS}$ ) versus EC measured ( $G_{EC}$ ) soil heat flux.

5

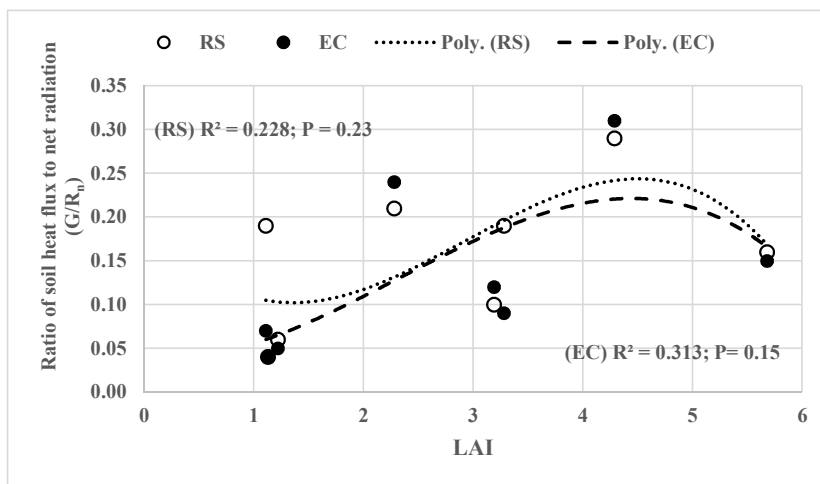
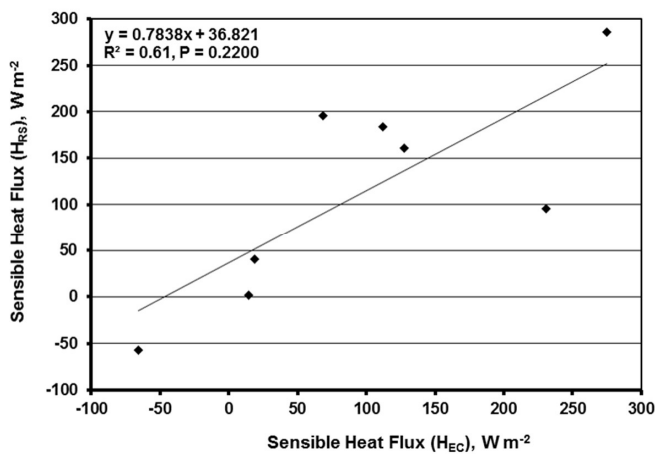


**Figure 6.** LAI and  $G/R_n$  relationship of the study crop for remote sensing and Eddy Covariance.



5

**Figure 7.** Comparison between the measured ( $H_{EC}$ ) and METRIC derived ( $H_{RS}$ ) sensible heat flux.

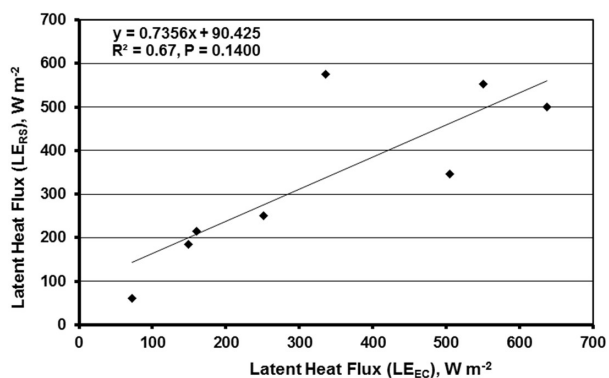


**Figure 8.** METRIC-derived hourly latent heat fluxes ( $LE_{RS}$ ) versus Eddy Covariance measurements ( $LE_{EC}$ ).

10

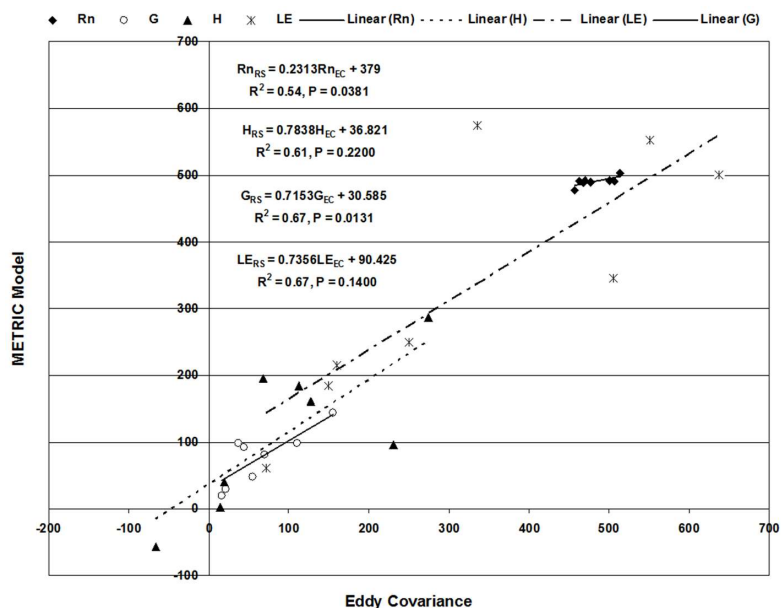


Figure 9. Relationship between EB components ( $W m^{-2}$ ) measured by the METRIC algorithm and the EC system.

5

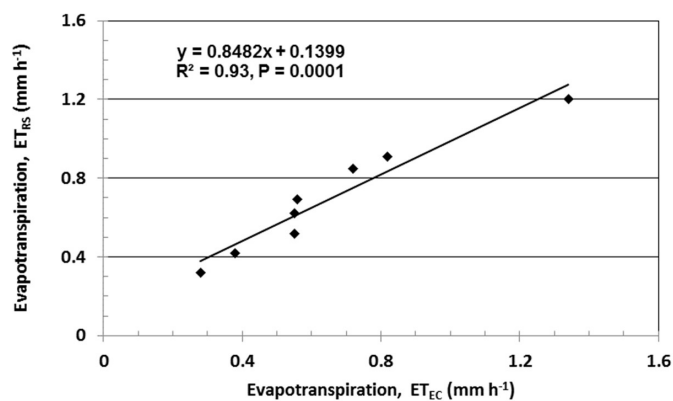


Figure 10. Relationship between the  $ET_{RS}$  and  $ET_{EC}$ .